JOC The Journal of Organic Chemistry

Article

pubs.acs.org/joc

Encapsulated Guests in the Smallest Spaces: Shrinking Guests by Compression and Investigations under Solvent-Free Conditions

Gebhard Haberhauer,* Sascha Woitschetzki, and Christof Füten

Institut für Organische Chemie, Universität Duisburg-Essen, Universitätsstr. 7, D-45117 Essen, Germany

Supporting Information

ABSTRACT: Noncovalent interactions play a pivotal role in a variety of biological and chemical processes. The experimental determination and quantum chemical calculations of the forces driving these interactions are of utmost importance. Of special interest are interactions of molecules in small spaces which show phenomena different from conventional behavior in solution. An extension is the encapsulation of guests in smallest spaces: The guests are too large to be included under standard conditions and hence must be forced to intrude into the cavity. Here, we show the design of such a host−guest system which allows to directly compare the measured thermodynamic values to gas-phase quantum chemical calculations. Structural investigation of the complexes reveals that the encapsulation process causes not only an extension of the hollow space of the host but also a shrinking of the included guest by compression.

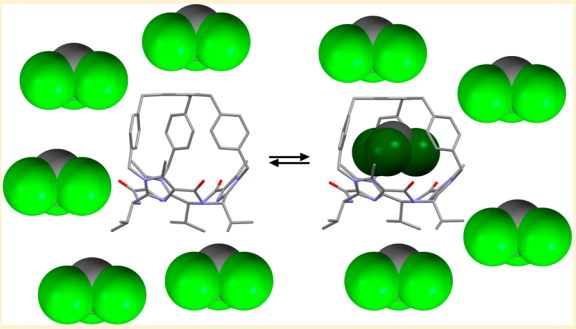

INTRODUCTION

Molecular recognition is a key step in a variety of biological and chemical processes. Therefore, it is of utmost importance to identify and quantify the intermolecular forces that drive this process. Of high interest are noncovalent host−guest interactions which are mainly dominated by London forces.[1] A well-known example for cage compounds[2] which include small nonpolar guests driven by dispersion interactions is the cryptophane family.[3] A variety of studies has been published concerning the reversible binding of cryptophane hosts to small nonpolar molecules.[3c] Numerous experimentally determined thermodynamic data for the encapsulation of nonpolar guests in cryptophane hosts are available.[4,3c] Also a number of computational studies on cryptophanes are published,[3c,5] but astonishingly only few of them deal with the energies of the inclusion process.[5c,6] The calculated data in these studies show a striking difference to experimentally determined values.[6] This is mainly *not* due to imprecise quantum chemical calculations: During the past decade computers have become more powerful allowing to calculate even larger systems (>100 atoms) using highly sophisticated methods including dispersion corrections and medium-range basis sets. That means, the complex formation energy of a van der Waals complex in the gas phase can be calculated with high levels of precision. The nonconformity of calculated and measured data can also be due to experimental factors. One serious problem is the fact that experimentally determined values do not exactly reflect the thermodynamic data of the inclusion process, as they include a series of side processes. One of the most interfering factors in measuring the free enthalpy of encapsulation is the solvent.[1c−e] This is valid for calculations using quantum chemical approximations as well as for the experiments. In the case of the calculations in solution, the method used has to consider all interacting forces of the solvent with the reactants and the products. However, the method should yield reliable results within a reasonable computing time. In case of the experiments, the release of encapsulated solvent can be an exothermic or endothermic process resulting in a deviation of the measured enthalpy from the inclusion enthalpy of the guest.[1c,7,1e] In order to avoid this side process, solvents which are too large to be included are often used. However, it has been shown that solvents can penetrate into cavities which were thought to be too small for them.[3c,8] This problem has often been overlooked as it is generally not trivial to prove the inclusion of a solvent molecule when working in a solution of this solvent. Furthermore, in some cases implosion of the empty container molecules[3c] is observed leading to a mixture of several equilibria.[8] These factors result in a large deviation between the measured thermodynamic data and the desired one. Hence, there is an extensive need for the design of systems which allows a better and more reliable comparison between experimentally obtained and calculated data. Ideally, the measured values could directly be compared to the calculation in the gas phase as well as in solution. This would allow to evaluate separately the gas-phase calculation and the model for the interactions in solution.

During the last years the concept of molecules in small spaces was introduced in supramolecular chemistry.[9,10] This studies the encapsulation of guests into spaces barely big

Received: May 27, 2015
Published: July 28, 2015

ACS Publications © 2015 American Chemical Society

DOI: 10.1021/acs.joc.5b01187
J. Org. Chem. 2015, 80, 8065−8072

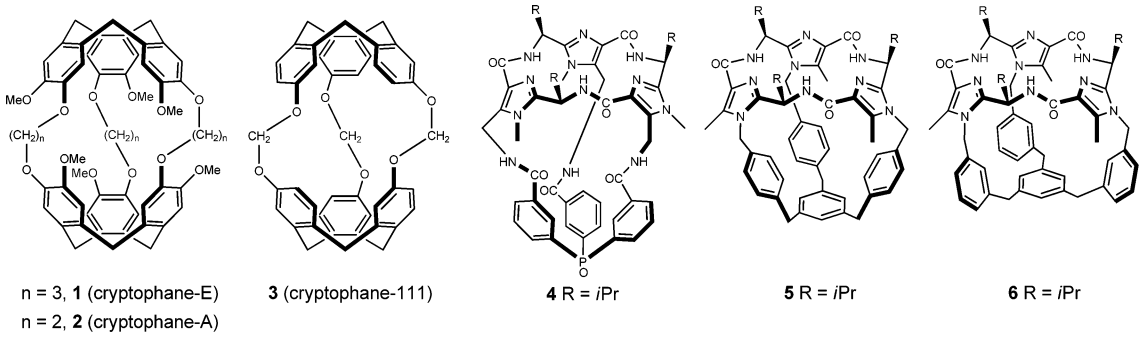

Figure 1. Structures of cryptophanes **1**–**3** and the imidazole-containing containers **4**–**6**.

Scheme 1. Synthesis of the Imidazole Containers 5 and 6[a]

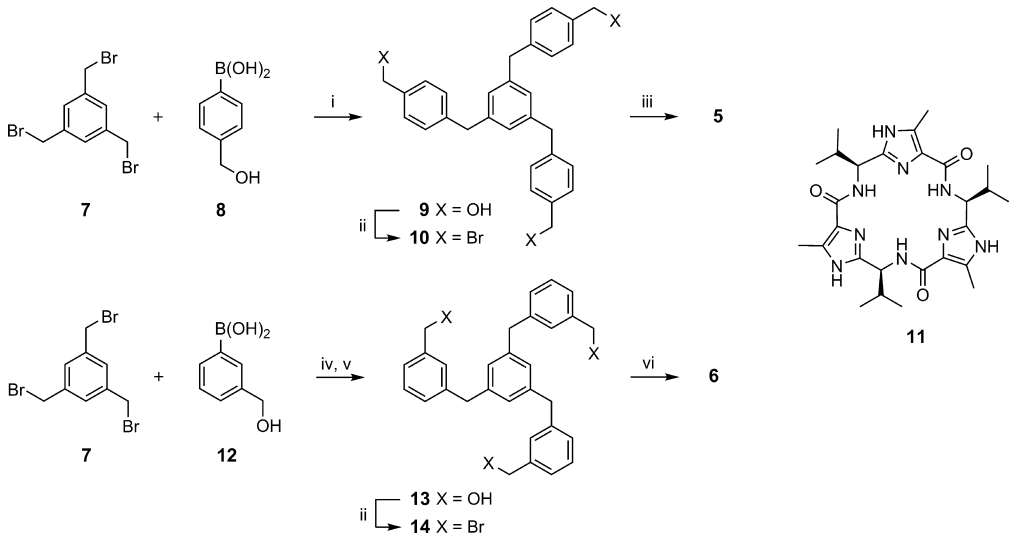

[a]Reaction conditions: (i) $Pd(PPh_3)_4$, K_2CO_3, dioxane, Δ, 68%. (ii) PPh_3, *N*-bromosuccinimide, tetrahydrofuran, 0 °C, 95%. (iii) **11**, Cs_2CO_3, acetonitrile, Δ, 46%. (iv) $Pd(PPh_3)_4$, K_2CO_3, dioxane, Δ, 64%. (v) PPh_3, *N*-bromosuccinimide, tetrahydrofuran, 0 °C, 73%. (vi) **11**, Cs_2CO_3, acetonitrile, Δ, 46%.

enough to contain them. These guests show reduced mobilities[9c] such as rotation and translation within the host. There are examples where flexible structures such as normal alkanes can be compressed to fit within the hosts and conform to their shapes.[9a,b]

We want to extend the concept of molecular recognition in small spaces to inclusion into smallest spaces. The guests are too big to be encapsulated under standard conditions and must be forced to enter the cavity ($\Delta G_{incl} > 0$). To observe the complex formation, a large excess of the guest must be used. This allows to work under solvent-free conditions, since the whole phase consists only of the host and the guest. As mentioned above, guest molecules encapsulated in small spaces show a special behavior.[9a,b,d] Therefore, the investigation of the structural changes of guest and host caused by encapsulation in smallest spaces is—beside the comparison of measured and calculated data—an additional incentive for developing these systems.

Here we show the design of a container molecule which encapsulates a guest molecule under solvent-free conditions in such a way that the thermodynamic parameters of the corresponding complexes can be measured and then directly compared with the quantum chemical calculations in gas phase as well as in solution. In these complexes the guests are encapsulated in smallest spaces, which leads to an extension of the cavity of the host and to a shrinking of the volume of the guest molecule.

RESULTS AND DISCUSSION

Concept. An investigation under solvent-free conditions means that the examined (liquid) phase consists only of the host and the guest. For encapsulation in smallest spaces the concentration of the guest molecule must be much higher (>1000-fold) than the concentration of the host molecule. The guest is required to be liquid over a large range of temperatures, thus allowing to measure the equilibrium over a wide range. This is necessary to determine accurately the enthalpy and entropy of inclusion. Furthermore, it is important that the host does not strongly change its external shape during the inclusion process; that means the empty container must not implode.

Let us consider the equilibrium between the container, the guest, and the complex under the above-mentioned requirements. As the study is carried out in liquid phase, the measurement delivers the enthalpy of inclusion in liquid phase ($\Delta H_{incl,liquid\ phase}$). This consists of the enthalpy of inclusion in the gas phase ($\Delta H_{incl,gas\ phase}$) as well as the enthalpies of solution for the container, the guest, and the complex according to eq 1. Due to the above-mentioned requirements, the container must not implode, and therefore the enthalpies of solution for the container ($\Delta H_{solv}^{container}$) and for the complex

DOI: 10.1021/acs.joc.5b01187
J. Org. Chem. 2015, 80, 8065–8072

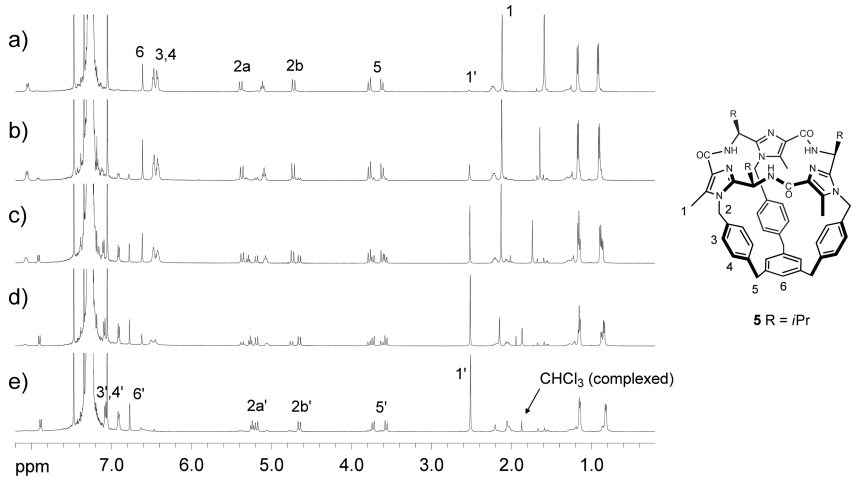

Figure 2. ^{1}H NMR spectra of **5** at 500 MHz in $CHCl_3/CDCl_3$ (10/1) at 298 K (a), 278 K (b), 258 K (c), 238 K (d), and 218 K (e).

($\Delta H_{solv}^{complex}$) are, in a first approximation, of equal size. Thus, the term $\Delta H_{solv}^{complex} - \Delta H_{solv}^{container}$ in eq 1 can be dropped, and we obtain eq 2 in which beside the enthalpy of inclusion in the gas phase ($\Delta H_{incl,gas\ phase}$) only the term ΔH_{solv}^{guest} occurs. As we consider solvent-free conditions in which the concentration of the guest is more than 1000-fold higher than the concentration of the host, the enthalpy of solution of the guest is nothing else than the negative value of the enthalpy of evaporation of the guest (ΔH_{vap}^{guest}), eq 3, which is listed for a variety of liquids.[11] Consequently, the enthalpy of inclusion in the gas phase ($\Delta H_{incl,gas\ phase}$) can be calculated from the enthalpy of inclusion in the liquid phase ($\Delta H_{incl,liquid\ phase}$) and the enthalpy of evaporation of the guest (ΔH_{vap}^{guest}) according to eq 4:

$$\Delta H_{incl,liquid\ phase} = \Delta H_{incl,gas\ phase} + \Delta H_{solv}^{complex} - \Delta H_{solv}^{container} - \Delta H_{solv}^{guest} \quad (1)$$

$$= \Delta H_{incl,gas\ phase} - \Delta H_{solv}^{guest} \quad (2)$$

$$= \Delta H_{incl,gas\ phase} + \Delta H_{vap}^{guest} \quad (3)$$

$$\Delta H_{incl,gas\ phase} = \Delta H_{incl,liquid\ phase} - \Delta H_{vap}^{guest} \quad (4)$$

This allows us to determine the enthalpy of inclusion in the gas phase ($\Delta H_{incl,gas\ phase}$) without disturbing side processes of the solvent and compare it directly with the calculations in the gas phase. Furthermore, the comparison of the enthalpies of inclusion in the liquid phase ($\Delta H_{incl,liquid\ phase}$) enables us to separately evaluate the quantum chemical solution models.

For our approach we used chloroform as guest, because there are already some containers described in the literature which are able to form stable complexes with chloroform based on dispersion interactions.[12,4b,6,8] Furthermore, chloroform is C_3-symmetric which makes the interpretation and analysis of the inclusion complex easier. As a starting point cryptophanes **1**[13,4a] and **2**[21] as well as the imidazole container **4**[15] were chosen (Figure 1). All of them are known to form very stable chloroform complexes. To investigate the encapsulation of chloroform in smallest spaces, we looked for containers with a smaller cavity. As candidates we chose cryptophane-111[13] (**3**) and the two imidazole-containing containers **5** and **6**.

Syntheses and Proof of Encapsulation of $CHCl_3$. The syntheses of the cryptophanes were conducted according to known procedures.[3b] The synthesis of the containers **5** and **6** is depicted in Scheme 1. As a starting material, the commercially available tribromide **7** and the imidazole-containing cycle **11** were used. Starting from tribromide **7** the triols **9** and **13** are prepared, and the latter can be transformed into the tribromides **10** and **14** using triphenylphoshine and *N*-bromosuccinimide in tetrahydrofuran. An alkylation reaction of the tribromides **10** and **14** with the macrocycle **11**[14] leads to the desired containers **5** and **6**.

To prove the inclusion of chloroform into the containers **4**–**6** in chloroform, we first wanted to check which detection technique is suitable. As reference we used cryptophane-E (**1**) and cryptophane-A (**2**) which are known to bind chloroform at room temperature and under dilution.[13,21] The containers **1**–**3**, **5**, and **6** were dissolved in a mixture of $CHCl_3$ and $CDCl_3$ (10:1) at a millimolar concentration, and their NMR spectra were recorded at 218 K (Figure S1). This temperature was used as it is the lowest-possible measuring temperature for liquid chloroform. The use of a low temperature is reasonable, as the binding constants for van der Waals complexes are largest at low temperatures. Moreover, the inclusion proceeds slower at low temperatures which often allows to observe two separated signals for the free and the encapsulated chloroform. In the ^{1}H NMR spectra of the containers **1**, **2**, and **5** a signal for the included chloroform is observed at 218 K. For cryptophane **3** and container **6** no such signals are found. However, this does not necessarily mean that no chloroform is encapsulated. An unambiguous proof that the signals at 1.8–3.0 ppm indeed belong to the enclosed chloroform can be found in the corresponding 2D NMR spectra. In the ^{1}H–^{13}C COSY NMR spectra of **1**, **2**, and **5** a cross peak between the hydrogen of the complexed $CHCl_3$ and the carbon of the complexed $CHCl_3$ appears (Figures S2–S4). The latter is only slightly shifted to higher field compared to the signal for the free chloroform. In case of container **6**, no cross signal can be observed in the ^{1}H–^{13}C COSY NMR spectrum (Figure S5).

If the samples are warmed up to room temperatures, no significant changes are observed in the ^{1}H NMR spectra of the cryptophanes **1**–**3** and the container **6** (Figure S6). In case of container **5**, a second set of signal appears at higher temperatures, and the signal of the enclosed chloroform disappears (Figure 2). This is a hint for the exclusion of chloroform from the cavity with increasing temperature resulting in a mixture of empty and filled container. At higher temperatures (>298 K) only the empty container is present in solution.

DOI: 10.1021/acs.joc.5b01187
J. Org. Chem. 2015, 80, 8065–8072

This assumption is corroborated by three proofs. First, the chemical shifts of the protons H3 and H4 are found at 6.4 and 6.5 ppm at higher temperatures (Figure 2). This indicates that they belong to the empty container and partially protrude inside the cavity which causes the highfield shift of these aromatic protons. At lower temperatures the signals of the protons H3′ and H4′ appear at 7.0−7.1 ppm which indicates that the cavity is now filled, and the protons H3′ and H4′ are not located in the cavity. It has to be noted that both in the empty and in the filled container the rotation of the *para*-phenylene units is fast compared to the NMR time scale. Second, the ^{1}H NMR spectra of container **5** in 1,1,2,2-tetrachloroethane ($C_2D_2Cl_4$) are almost independent of the measuring temperature. $C_2D_2Cl_4$ is too large to fit into the cavity of container **5** (Figure S7), and the signals of the protons H3 and H4 are found at 6.4 and 6.5 ppm which resembles the values found for the chemical shifts of H3 and H4 in $CHCl_3$ at higher temperatures. Third, container **5** can also encapsulate $CHBrCl_2$ at low temperatures (Figures S8) which can be seen by a highfield shift of the proton of $CHBrCl_2$ (1.9 ppm) and the appearance of further signals for the complex $CHBrCl_2$@**5**. As the latter one is not C_3-symmetric and as the rotation of the guest within the cavity is slow, the signals of $CHBrCl_2$@**5** are broad. The number of new signals indicates that the rotation of the *para*-phenylene units in complex $CHBrCl_2$@**5** is slow compared to the NMR time scale. This difference toward the complex $CHCl_3$@**5** seems consequential as $CHBrCl_2$ is larger than $CHCl_3$. Here again, the inclusion can be proven by the ^{1}H−^{13}C COSY NMR spectrum of $CHBrCl_2$@**5**, where a cross peak between the hydrogen of the complexed $CHBrCl_2$ and the carbon of the complexed $CHBrCl_2$ appears (Figures S9). The latter is only slightly shifted to a higher field compared to the signal for the free $CHBrCl_2$.

The enclosed chloroform in $CHCl_3$@**5** can in principle adopt two orientations: On the one hand the proton of $CHCl_3$ can point toward the cup-shaped cyclopeptide, and on the other hand it can point toward the benzene unit. In the following the first (second) orientation is labeled with the symbol ↑ (↓). In the previously reported complex $CHCl_3$@**4** the proton of the chloroform points toward the cup-shaped cyclopeptide, as proven by a cross signal in the NOESY spectrum of $CHCl_3$@**4** and by a highfield shift of 2.1 ppm.[6] In the now investigated complex $CHCl_3$@**5** no cross peak between the chloroform and the amide protons are found, and the observed highfield shift is much larger (5.4 ppm). This suggests that the proton of the encapsulated chloroform is directly located over the center of a benzene unit which is the case for complex ↓$CHCl_3$@**5**.

The occurrence of separate signals for the empty container **5** and the complex ↓$CHCl_3$@**5** over a large range of temperatures allows the determination of the thermodynamic parameters of the inclusion process. A further advantage of solvent-free conditions is the fact that the concentration of the guest is more than 1000-fold higher than the concentration of the host which makes the concentration of the guest to a *defacto* constant term. Thus, the ratio between the empty container **5** and the complex ↓$CHCl_3$@**5** is independent of the concentration of the host under these conditions. This decrease of possible error sources makes the data obtained by ^{1}H NMR techniques more accurate.

For the determination of the thermodynamic parameters several independent series of measurements were performed. One of them is depicted in Figure 3. For the enthalpy of inclusion in the liquid phase ($\Delta H^{238-288}_{\text{incl,liquid phase}}$) a value of −7.6 ± 0.3 kcal mol^{-1} was obtained. The entropy of inclusion in the liquid phase ($\Delta S^{238-288}_{\text{incl,liquid phase}}$) was measured to be −36 ± 1 cal mol^{-1} K^{-1}. To obtain the enthalpy of inclusion in the gas phase ($\Delta H^{238-288}_{\text{incl,gas phase}}$) the enthalpy of vaporization of the guest $\Delta H^{\text{guest},238-288}_{\text{vap}}$ has to be subtracted from this term. The enthalpy of vaporization $\Delta H^{\text{guest},238-288}_{\text{vap}}$ can be calculated from the listed enthalpy of vaporization at 298 K (7.50 kcal mol^{-1})[11] and the heat capacity (C_p)[11] according to eq 5:

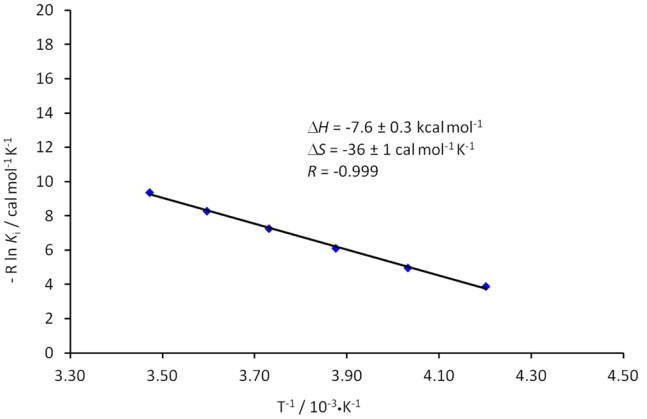

Figure 3. Thermodynamic parameters of ↓$CHCl_3$@**5** in $CHCl_3$/$CDCl_3$ (10/1). Plot of $-R^* \ln K_i$ against $1/T$ in the area of 238−288 K. $\Delta H^{238-288}_{\text{incl,liquid phase}} = -7.6 \pm 0.3$ kcal mol^{-1}, $\Delta S^{238-288}_{\text{incl,liquid phase}} = -36 \pm 1$ cal mol^{-1} K^{-1}, and $R = -0.999$.

$$\Delta H^{\text{guest},T}_{\text{vap}} = \Delta H^{\text{guest},298}_{\text{vap}} + C_p \times (298 - T) \quad (5)$$

In an analogous procedure the entropy of the inclusion in the gas phase can be calculated from the entropy of the inclusion in the liquid phase and the entropy of vaporization of chloroform. The latter is obtained by the difference between the entropy of chloroform in the gas phase and in the liquid phase.[11] Here again, using eq 6 a mean value for the temperature range from 238 to 288 K can be calculated.

$$S^T = S^{298} + C_p \times \ln\left(\frac{T}{298}\right) \quad (6)$$

Applying this methodology the following values are obtained for the formation of the complex ↓$CHCl_3$@**5** in the gas phase: $\Delta H^{238-288}_{\text{incl,gas phase}} = -16.0 \pm 0.3$ kcal mol^{-1}, $\Delta S^{238-288}_{\text{incl,gas phase}} = -60 \pm 1$ cal mol^{-1} K^{-1}. These values can now directly be compared to the calculations in the gas phase.

Calculations of the Interaction Energies of the Host−Guest Complexes. All calculations were performed by using the program package Gaussian 09[15] and TURBOMOLE.[16] The molecular structures were fully optimized in the gas phase using the DFT potential B3LYP-D3[17−19] which includes an additional dispersion correction.[20,21] Two different basis sets were employed. The first is a combination of two basis sets and will be further referred to as 6-31G*,cc-pVTZ. For the light elements C, N, O, and H, the 6-31G*[22] basis set was used, whereas for the halogens Cl and Br the cc-pVTZ[23] basis set was employed. As second basis set the def2-TZVP[24] basis has been used. For all stationary points no symmetry restriction was applied. Frequency calculations by means of B3LYP-D3/6-31G*,cc-pVTZ were carried out at each of the structures to verify the nature of the stationary point. In all cases, no imaginary frequencies were found. For the computation of the internal entropies, the procedure suggested by Grimme has been employed.[21] In this approach the contribution of the low-

DOI: 10.1021/acs.joc.5b01187
J. Org. Chem. 2015, 80, 8065−8072

lying modes to the entropy is replaced by a corresponding rotational entropy (quasi-RRHO approach). We used the same values for ω_0 and B_{av} as suggested in the literature.[21]

The single point energies of the geometry optimized structures of chloroform, the empty container **5**, and the complex ↓$CHCl_3$@**5** were calculated using a variety of DFT potentials.[15,16] Some of them cover mid-range and long-range correlation. Furthermore, single point calculations for $CHCl_3$, **5** and ↓$CHCl_3$@**5** were performed by means of the double hybrid method B2PLYPD[25] by Grimme. To calculate the enthalpy and entropy of association in solution, the continuum solvation models COSMO,[26] SMD,[27] and COSMO-RS[28] were employed. All data are summarized in Tables 1 and 2, and the calculated structures are depicted in Figures 4 and S10−S15.

Table 1. Interaction Energy (ΔE in kcal mol^{-1}), Enthalpy ($\Delta H^{238-288}$ in kcal mol^{-1}), and Entropy ($\Delta H^{238-288}$ in cal mol^{-1} K^{-1}) for the Complex Formation of ↓$CHCl_3$@5**[a]**

method	phase	ΔE	$\Delta H^{238-288}$	$\Delta S^{238-288}$
experiment	gas		−16.0 ± 0.3	−60 ± 1
B3LYP-D3	gas	−18.4	−16.9	−51
B3LYP-D2	gas	−16.4	−14.8	
B3LYP	gas	+15.3	+16.8	
B97-D3	gas	−15.7	−14.2	
B97D	gas	−2.5	−1.0	
TPSS-D3	gas	−14.7	−13.1	
TPSS-D2	gas	−15.9	−14.4	
TPSS	gas	+14.2	+15.8	
TPSSH-D3	gas	−14.7	−13.2	
TPSSH	gas	+13.3	+14.9	
PBE0-D3	gas	−15.0	−13.4	
PBE0	gas	+7.0	+8.5	
wB97XD	gas	−14.8	−13.2	
PW6B95-D3	gas	−16.7	−15.2	
M05-2X	gas	−12.0	−10.4	
M06-2X	gas	−19.3	−17.7	
M06	gas	−21.1	−19.6	
B2PLYPD	gas	−19.5	−17.9	
experiment	liquid		−7.6 ± 0.3	−36 ± 1
B3LYP-D3 − COSMO-RS	liquid	−10.3	−8.8	
B3LYP-D3 − COSMO	liquid	−16.2	−14.7	
B3LYP-D3 − SMD	liquid	−7.3	−5.8	

[a]All structures were optimized by means of B3LYP-D3/def2-TZVP. Based on these structures, single point calculations by means of different quantum chemical methods were carried out using the def2-TZVP basis set. The internal entropies were calculated following the procedure by Grimme[21] based on frequency analysis by means of B3LYP-D3/6-31G*,cc-pVTZ.

In order to determine the change in the volume of the internal cavities of the hosts **1**−**6** caused by inclusion of $CHCl_3$ and $CHBrCl_2$, we calculated the volume of the cavities of the empty (V_{empty}) as well as filled (V_{filled}) containers **1**−**6** by means of MSROLL.[29] The geometries were taken from the B3LYP-D3/def2-TZVP calculations. The data are summarized in Table 2. A glance shows that the volumes of the container molecules **1**−**6** range between 25 and 114 Å^3. These volumes are within the range of Rebek's tennis ball (69 Å^3)[30] and softball (313 Å^3),[30] but rather small compared to the inner volumes found in oligomeric assemblies of deep-cavity cavitands (500−3700 Å^3) by Gibb et al.[31] The volume of the internal cavities of the hosts **3**, **5**, and **6** is smaller than the volume of the guest molecules $CHCl_3$ (72 Å^3)[13] and $CHBrCl_2$ (76 Å^3).[4a]

A comparison of the calculated enthalpies of the complex ↓$CHCl_3$@**5** in the gas phase with the experimentally determined inclusion enthalpy in the gas phase $\Delta H^{238-288}_{incl,gas\ phase}$ shows that they are in good to very good agreement when the dispersion interactions are considered (Table 1). Without dispersion correction, the calculated energies deviate from the measured one by more than 30 kcal mol^{-1} (Table 1). The best matches are obtained by using DFT potentials with the additional dispersion correction D3. For the best methods (PW6B95-D3 and B3LYP-D3) the deviation from the experiment is smaller than 1 kcal mol^{-1}.

A comparison of the calculated enthalpies of the complex ↓$CHCl_3$@**5** in the liquid phase with the experimentally determined inclusion enthalpy in the liquid phase $\Delta H^{238-288}_{incl,liquid\ phase}$ reveals that the COSMO-RS approximation delivers the best result within the solvent models used. Here again the deviation from the experimental data is smaller than 1 kcal mol^{-1}.

A comparison of the formation energies (B3LYP-D3/def2-TZVP) of the complexes ↑$CHCl_3$@**5** and ↓$CHCl_3$@**5** shows (Table 2 and Figure 4) that ↓$CHCl_3$@**5** is about 2 kcal mol^{-1} more stable than its stereoisomer. According to the Boltzmann distribution the ratio between the isomers ↓$CHCl_3$@**5** and ↑$CHCl_3$@**5** amounts to 100:3 at 218 K. This coincides with the experimental ^{1}H NMR data which indicate the sole presence of ↓$CHCl_3$@**5** in solution at 218 K. The same preference is found for the complex $CHBrCl_2$@**5**. For container **6** an inverse stability of the complexes is found. Due to the low formation energies of the complexes of ↑$CHCl_3$@**6** and $CHCl_3$@cryptophane-111 (−11.0 and −11.6 kcal mol^{-1}), it can be assumed that no inclusion process proceeds within the examined range of temperatures. It has to be noted that the calculated formation energy of the complex ↓$CHCl_3$@**5** amounts to −18.4 kcal mol^{-1}, and the encapsulation is only observed at temperatures below 298 K. Although $CHBrCl_2$ is larger than $CHCl_3$, the calculated values are in the same range (Table 2). This is probably due to the fact that the larger repulsive interactions are compensated by the larger dispersion interactions of the bromine atom with the atoms of the cavity.

As mentioned in the Introduction section, one fascinating aspect for encapsulation in smallest spaces is the question of how inclusion changes the form and size of both the host and the guest. Table 2 shows that inclusion of chloroform into the cryptophanes **1** and **2** and into container **3** leads to only a small change in the volume of the internal cavities of these hosts. For the containers **5** and **6** an extension of the hollow space of more than 48 Å^3 is found. How tightly the guest fits inside the cavity can be seen when the space-fill models of the calculated structures are considered. While the chloroform molecule lightly touches the atoms of the cavity in the complexes $CHCl_3$@cryptophane-E and $CHCl_3$@cryptophane-A, there is a significant overlap of the electron clouds of the guests and the atoms of the imidazole units in the complexes ↓$CHCl_3$@**5** and ↓$CHBrCl_2$@**5** (Figures S14−S16). This can also be seen in the plotted electron density distribution. Here the question arises which structural effect on the guests is caused by encapsulation in smallest spaces and how this effect can be detected. An assumption is that this encapsulation leads to a compression of the whole molecule resulting in a decreased molecule. A quantum chemical consideration of this compression is difficult as there is no definition where one molecule ends and the other

DOI: 10.1021/acs.joc.5b01187
J. Org. Chem. 2015, 80, 8065−8072

Table 2. Calculated Gas-Phase Interaction Energies ΔE_i [kcal mol^{-1}], Volume of the Internal Cavities of the Empty (V_{empty} [Å^3]) and Filled (V_{filled} [Å^3]) Containers, the Changes in Volume of the Cavity of the Hosts ΔV [Å^3], and Changes in the Bond Lengths of the Guests Δr [pm] for the Host–Guest Complexes of the Containers 1–6 with $CHCl_3$ and $CHBrCl_2$[a]

complex	ΔE	V_{empty}	V_{filled}	ΔV	Δr (H)	Δr (Cl)	Δr (Br)
$CHCl_3$@**1**	−22.7	111.2[a]	126.6[a]	+15.4[a]	+0.2	−0.2	
$CHCl_3$@**2**	−24.0	101.0[b]	105.1[b]	+4.1[b]	+0.0	−0.3	
$CHCl_3$@**3**	−11.6	57.8[b]	−[c]	−[c]	−0.1	−1.0	
↑$CHCl_3$@**4**	−25.8	114.0[d]	116.1[d]	+2.1[d]	+0.2	−0.2	
↑$CHCl_3$@**5**	−16.9	49.6[a]	97.8[a]	+48.2[a]	+0.2	−0.5	
↓$CHCl_3$@**5**	−18.4	49.6[a]	97.7[a]	+48.1[a]	−0.5	−0.6	
↑$CHBrCl_2$@**5**	−16.9	45.0[d]	95.6[d]	+50.6[d]	+0.2	−0.4	−1.3
↓$CHBrCl_2$@**5**	−18.3	49.6[d]	100.1[d]	+50.5[a]	−0.4	−0.5	−1.5
↑$CHCl_3$@**6**	−11.0	24.6[a]	93.3[a]	+68.7[a]	+0.2	−0.5	
↓$CHCl_3$@**6**	−9.4	24.6[a]	97.0[a]	+72.4[a]	−0.8	−0.8	

[a]In the orientation ↑ (↓) the chloroform proton points toward (away from) the amide protons of the cup-shaped azole-containing cyclopeptide. [b]A probe of 1.40 Å diameter was used. [c]A probe of 1.45 Å diameter was used. [d]No cavity was found. [e]A probe of 1.50 Å diameter was used.

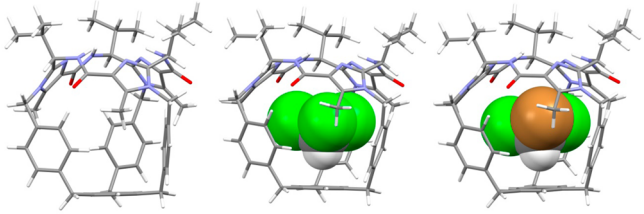

Figure 4. Molecular structures of container **5** (left) as well as the complexes ↓$CHCl_3$@**5** (middle) and ↓$CHBrCl_2$@**5** (right) calculated using B3LYP-D3/def2-TZVP.

one begins, especially if there is an overlap of the electron densities. In other words, the compression of the guest molecule cannot easily be determined by considering the electron density. However, the compression should indirectly influence the nucleus–nucleus distances. If the compression of the electron cloud is large enough, the nucleus–nucleus distances should also be reduced. Indeed, the calculations show that there are no significant changes in the nucleus–nucleus distances of the guest molecules (Δr) in the standard complexes ($CHCl_3$@**1**, $CHCl_3$@**2**, and $CHCl_3$@**4**; Table 2). However, in the complexes ↓$CHCl_3$@**5** and ↓$CHBrCl_2$@**5**, in which the guests are included in smallest spaces, a reduction of the C–Cl and C–Br distances is found. The highest decrease of a bond (Δr = −1.5 pm; 0.8%) is calculated for the complex ↓$CHBrCl_2$@**5**.

CONCLUSION

In summary, we were able to design a container molecule for the inclusion of guests in smallest spaces. The encapsulation process was investigated under solvent-free conditions, and the enthalpy as well as entropy of the inclusion were determined. The special concept of encapsulation in smallest spaces allows to directly compare the measured values to gas-phase quantum chemical calculations. The observed deviation between experiment and the best calculation results is smaller than 1 kcal mol^{-1}. The structural investigation of the complexes of this container with chloroform and bromodichloromethane shows that the guests are extremely tightly bound in the hollow space. The encapsulation process results in an extension of the volume of the cavity of the host and in a shrinking of the included guests. The latter becomes manifested by the decrease of the C–Cl and C–Br distances.

EXPERIMENTAL SECTION

General Remarks. All chemicals were reagent grade and were used as purchased. Reactions were monitored by TLC analysis with silica gel 60 F254 thin-layer plates. Flash chromatography was carried out on silica gel 60 (230–400 mesh). ^{1}H, ^{13}C NMR, and 2D NMR spectra were recorded on 500 and 600 MHz spectrometers. All chemical shifts (δ) are given in ppm. The spectra were referenced to the peak for the protium impurity in the deuterated solvents indicated in brackets in the analytical data. HR-MS spectra were recorded using a time-of-flight detector.

Synthesis of Triol 9. 1,3,5-Tris(bromomethyl)benzene (**7**; 178 mg, 0.50 mmol) and 4-hydroxymethylbenzene boronic acid (**8**; 456 mg, 3.00 mmol) were dissolved in dioxane (10 mL) under an argon atmosphere. $Pd(PPh_3)_4$ (58 mg, 0.05 mmol) and an aqueous solution of potassium carbonate (saturated; 1.0 mL) were added to the solution. The reaction mixture was warmed to 80 °C and stirred at that temperature overnight. After cooling to room temperature, dichloromethane (60 mL) and water (10 mL) were added. The phases were separated, and the aqueous layer was extracted several times with dichloromethane. The organic layers were combined and dried over $MgSO_4$, the solvent was removed, and the crude product was purified by column chromatography over silica gel (dichloromethane/ethyl acetate/methanol 75:25:5) to give **9** (150 mg, 0.34 mmol, 68%) as a white solid. Mp: 142–143 °C. ^{1}H NMR (600 MHz, CD_3OD): δ = 7.22 (d, $^3J_{H,H}$ = 8.0 Hz, 6 H, H_{ar}), 7.10 (d, $^3J_{H,H}$ = 8.0 Hz, 6 H, H_{ar}), 6.84 (s, 3 H, H_{ar}), 4.54 (s, 6 H, CH_2), 3.84 (s, 6 H, CH_2) ppm. ^{13}C NMR (151 MHz, CD_3OD): δ = 143.0, 141.9, 140.3, 129.9, 128.4, 128.3, 65.1, 42.4 ppm. HRMS (ESI+) $[C_{30}H_{30}O_3 + Na]^+$: calcd: 461.2093; observed: 461.2092. IR (ATR): 3271, 3054, 3023, 2910, 2864, 2839, 2439, 1915, 1808, 1597, 1513, 1454, 1420, 1366, 1317, 1269, 1214, 1203, 1183, 1108, 1028, 1010, 977, 953, 932, 865, 847, 808, 744, 700, 690 cm^{-1}. UV–vis (CH_3CN): absorption without local maxima.

Synthesis of Tribromide 10. Triol **9** (92 mg, 0.21 mmol) was dissolved in tetrahydrofuran (absolute; 25 mL) under an argon atmosphere. Triphenylphoshine (328 mg, 1.25 mmol) and *N*-bromosuccinimide (222 mg, 1.25 mmol) were added to the solution at 0 °C. The mixture was stirred at that temperature overnight. Subsequently, the solvent was removed, and the crude product was purified by column chromatography over silica gel (dichloromethane/*n*-hexane 1:1) to give **10** (125 mg, 0.20 mmol, 95%) as a white solid. Mp: 123–124 °C. ^{1}H NMR (600 MHz, $CDCl_3$): δ = 7.30 (d, $^3J_{H,H}$ = 8.0 Hz, 6 H, H_{ar}), 7.11 (d, $^3J_{H,H}$ = 8.0 Hz, 6 H, H_{ar}), 6.84 (s, 3 H, H_{ar}), 4.49 (s, 6 H, CH_2), 3.88 (s, 6 H, CH_2) ppm. ^{13}C NMR (125 MHz, $CDCl_3$): δ = 141.5, 141.0, 135.5, 129.23, 129.15, 127.59, 41.4, 33.6 ppm. HRMS (ESI+) $[C_{30}H_{27}{}^{79}Br_2{}^{81}Br + Na]^+$: calcd: 648.9540; observed: 648.9479. IR (ATR): 3126, 3091, 3049, 3017, 2939, 2916, 2850, 1908, 1796, 1598, 1511, 1455, 1435, 1418, 1227, 1200, 1125, 1093, 1020, 968, 935, 907, 890, 867, 824, 775, 763, 751, 732, 704 cm^{-1}. UV–vis (CH_3CN): λ_{max} (log ε) = 237 (4.74) nm.

DOI: 10.1021/acs.joc.5b01187
J. Org. Chem. 2015, 80, 8065–8072

Synthesis of Container 5. Cesium carbonate (650 mg, 2.00 mmol) was added to a solution of imidazole-containing cyclopeptide **11** (50 mg, 0.090 mmol) and tribromide **10** (70 mg, 0.110 mmol) in anhydrous acetonitrile (40 mL), and the mixture was refluxed at 90 °C for 4 h under an argon atmosphere. After cooling to room temperature, dichloromethane (60 mL) and water (15 mL) were added. The organic layer was washed with water, dried over $MgSO_4$, and concentrated in vacuo. Column chromatography of the residue on silica gel (dichloromethane/ethyl acetate, 3/1) provided compound **5** (38 mg, 0.041 mmol, 46%) as a white solid. The container is soluble in methanol and under high dilution condition also in methanol/water: 95/5. Mp: 214−216 °C. ^{1}H NMR (600 MHz, $C_2D_2Cl_4$): δ = 8.05 (d, $^3J_{H,H}$ = 9.6 Hz, 3 H, N*H*), 6.60 (s, 3 H, H_{ar}), 6.50 (d, $^3J_{H,H}$ = 7.3 Hz, 6 H, H_{ar}), 6.40 (d, $^3J_{H,H}$ = 7.4 Hz, 6 H, H_{ar}), 5.35 (d, $^2J_{H,H}$ = 16.0 Hz, 3 H, CH_2), 5.07 (t, $^3J_{H,H}$ = 9.2 Hz, 3 H, C*H*), 4.75 (d, $^2J_{H,H}$ = 16.1 Hz, 3 H, CH_2), 3.80 (d, $^2J_{H,H}$ = 14.8 Hz, 3 H, CH_2), 3.63 (d, $^2J_{H,H}$ = 14.7 Hz, 3 H, CH_2), 2.25−2.18 (m, 3 H, C*H*Me$_2$), 2.07 (s, 9 H, NCH_3), 1.15 (d, $^3J_{H,H}$ = 6.6 Hz, 9 H, CH_3), 0.92 (d, $^3J_{H,H}$ = 6.7 Hz, 9 H, CH_3) ppm. ^{13}C NMR (151 MHz, $C_2D_2Cl_4$): δ = 163.1, 148.9, 142.1, 141.7, 133.4, 131.7, 130.8, 128.6, 128.3, 126.0, 49.7, 46.9, 40.9, 35.0, 19.3, 19.1, 9.6 ppm. HRMS (ESI+) [$C_{57}H_{63}N_9O_3$ + H]$^+$: calcd: 922.5132; observed: 922.5127. IR (ATR): 3388, 2958, 2923, 2870, 1652, 1593, 1512, 1504, 1461, 1434, 1418, 1386, 1372, 1327, 1292, 1269, 1216, 1194, 1140, 1107, 1020, 1005, 949, 934, 917, 889, 821, 776, 742, 701, 654 cm^{-1}. UV−vis (CH_3CN): absorption without local maxima. CD (CH_3CN): λ_{max} ($\Delta\varepsilon$) = 204 (+177.11), 236 (−25.05), 241 (−10.14), 255 (−77.45), 271 (+4.53), 277 (+7.90 M^{-1} cm^{-1}) nm.

Synthesis of Triol 13. 1,3,5-Tris(bromomethyl)benzene (7; 178 mg, 0.50 mmol) and 3-hydroxymethylbenzene boronic acid (**12**; 456 mg, 3.00 mmol) were dissolved in dioxane (10 mL) under an argon atmosphere. $Pd(PPh_3)_4$ (58 mg, 0.05 mmol) and an aqueous solution of potassium carbonate (saturated; 1.0 mL) were added to the solution. The reaction mixture was warmed to 80 °C and stirred at that temperature overnight. After cooling to room temperature, dichloromethane (60 mL) and water (10 mL) were added. The phases were separated, and the aqueous layer was extracted several times with dichloromethane. The organic layers were combined and dried over $MgSO_4$, the solvent was removed, and the crude product was purified by column chromatography over silica gel (dichloromethane/ethyl acetate/methanol 75:25:5) to give **13** (141 mg, 0.32 mmol, 64%) as a white solid. Mp: 81−82 °C. ^{1}H NMR (600 MHz, $CDCl_3$): δ = 7.25 (t, $^3J_{H,H}$ = 7.5 Hz, 3 H, H_{ar}), 7.14 (d, $^3J_{H,H}$ = 7.6 Hz, 3 H, H_{ar}), 7.11 (d, $^3J_{H,H}$ = 7.6 Hz, 3 H, H_{ar}), 7.09 (s, 3 H, H_{ar}), 6.88 (s, 3 H, H_{ar}), 4.59 (s, 6 H, CH_2), 3.91 (s, 6 H, CH_2) ppm. ^{13}C NMR (151 MHz, $CDCl_3$): δ = 141.6, 141.2, 141.1, 128.5, 128.2, 127.6, 127.3, 124.6, 65.2, 41.7 ppm. HRMS (ESI+) [$C_{30}H_{30}O_3$ + Na]$^+$: calcd: 461.2093; observed: 461.2095. IR (ATR): 3288, 3021, 2916, 2850, 1597, 1487, 1440, 1426, 1361, 1233, 1219, 1149, 1086, 1050, 1031, 1007, 920, 883, 865, 796, 750, 727, 715, 700 cm^{-1}. UV−vis (CH_3CN): absorption without local maxima.

Synthesis of Tribromide 14. Triol **13** (70 mg, 0.16 mmol) was dissolved in tetrahydrofuran (absolute; 20 mL) under an argon atmosphere. Triphenylphoshine (247 mg, 0.94 mmol) and *N*-bromosuccinimide (167 mg, 0.94 mmol) were added to the solution at 0 °C. The mixture was stirred at that temperature overnight. Subsequently, the solvent was removed, and the crude product was purified by column chromatography over silica gel (dichloromethane/*n*-hexane 1:1) to give **14** (73 mg, 0.12 mmol, 73%) as a white solid. Mp.: 71−72 °C. ^{1}H NMR (600 MHz, $CDCl_3$): δ = 7.25−7.21 (m, 6 H, H_{ar}), 7.17 (s, 3 H, H_{ar}), 7.08 (d, $^3J_{H,H}$ = 7.2 Hz, 3 H, H_{ar}), 6.86 (s, 3 H, H_{ar}), 4.45 (s, 6 H, CH_2), 3.90 (s, 6 H, CH_2) ppm. ^{13}C NMR (125 MHz, $CDCl_3$): δ = 141.7, 141.0, 137.9, 129.5, 129.0, 128.9, 127.6, 126.8, 41.5, 33.7 ppm. HRMS (ESI+) [$C_{30}H_{27}{}^{79}Br_2{}^{81}Br$ + Na]$^+$: calcd: 648.9540; observed: 648.9589. IR (ATR): 3100, 3053, 3015, 2974, 2945, 2916, 2844, 1597, 1587, 1488, 1441, 1311, 1248, 1204, 1153, 1121, 1084, 1001, 976, 941, 909, 887, 853, 791, 759, 748, 713, 696, 675 cm^{-1}. UV−vis (CH_3CN): absorption without local maxima.

Synthesis of Container 6. Cesium carbonate (650 mg, 2.00 mmol) was added to a solution of imidazole-containing cyclopeptide **11** (50 mg, 0.090 mmol) and tribromide **14** (70 mg, 0.110 mmol) in anhydrous acetonitrile (40 mL), and the mixture was refluxed at 90 °C for 4 h under an argon atmosphere. After cooling to room temperature dichloromethane (60 mL) and water (15 mL) were added. The organic layer was washed with water, dried over $MgSO_4$, and concentrated in vacuo. Column chromatography of the residue on silica gel (dichloromethane/ethyl acetate, 3/1) provided compound **6** (25 mg, 0.041 mmol, 46%) as a white solid. The container is soluble in methanol and under a high-dilution condition also in methanol/water: 95/5. Mp: >350 °C. ^{1}H NMR (500 MHz, $C_2D_2Cl_4$): δ = 8.25 (d, $^3J_{H,H}$ = 9.9 Hz, 3 H, N*H*), 7.39 (t, $^3J_{H,H}$ = 7.6 Hz, 3 H, H_{ar}), 7.26 (d, $^3J_{H,H}$ = 7.8 Hz, 3 H, H_{ar}), 7.07 (d, $^3J_{H,H}$ = 7.5 Hz, 3 H, H_{ar}), 5.61 (s, 3 H, H_{ar}), 5.37 (d, $^2J_{H,H}$ = 17.0 Hz, 3 H, CH_2), 5.02 (t, $^3J_{H,H}$ = 9.0 Hz, 3 H, C*H*), 4.92 (d, $^2J_{H,H}$ = 17.0 Hz, 3 H, CH_2), 3.52 (s, 6 H, CH_2), 2.35 (s, 9 H, NCH_3), 2.19−2.12 (m, 3 H, C*H*Me$_2$), 1.11 (d, $^3J_{H,H}$ = 6.7 Hz, 9 H, CH_3), 0.99 (d, $^3J_{H,H}$ = 6.7 Hz, 9 H, CH_3) ppm. ^{13}C NMR (125 MHz, $C_2D_2Cl_4$): δ = 162.3, 148.1, 140.2, 139.9, 135.2, 130.4, 130.2, 129.5, 129.2, 126.8, 124.3, 124.1, 49.3, 46.4, 39.9, 35.0, 19.1, 18.9, 9.4 ppm. HRMS (ESI+) [$C_{57}H_{63}N_9O_3$ + H]$^+$: calcd: 922.5132; observed: 922.5127. IR (ATR): 3383, 3028, 2959, 2926, 2871, 1657, 1594, 1504, 1461, 1428, 1387, 1373, 1331, 1293, 1264, 1217, 1202, 1140, 1109, 1092, 1023, 951, 933, 918, 891, 874, 818, 785, 766, 740, 699, 653 cm^{-1}. UV−vis (CH_3CN): absorption without local maxima. CD (CH_3CN): λ_{max} ($\Delta\varepsilon$) = 219 (−126.63), 239 (−6.75), 252 (−78.77 M^{-1} cm^{-1}) nm.

■ ASSOCIATED CONTENT

Ⓢ Supporting Information

The Supporting Information is available free of charge on the ACS Publications website at DOI: 10.1021/acs.joc.5b01187.

NMR spectra and molecular structures of the container and complexes, Cartesian coordinates and absolute energies for all calculated compounds and complete ref 15 (PDF)

■ AUTHOR INFORMATION

Corresponding Author

*Email: gebhard.haberhauer@uni-due.de.

Notes

The authors declare no competing financial interest.

■ ACKNOWLEDGMENTS

This work was generously supported by the Deutsche Forschungsgemeinschaft (DFG). A special thank goes to Helma Kallweit and Petra Schneider.

■ REFERENCES

(1) (a) Vögtle, F.; Alfter, F. *Supramolecular Chemistry: An Introduction*; John Wiley & Sons: Chichester, 1993. (b) Lehn, J.-M. *Supramolecular Chemistry: Concepts and Perspectives*; VCH: Weinheim, 1995. (c) Steed, J. W.; Atwood, J. L. *Supramolecular Chemistry*; John Wiley & Sons: Chichester, 2000. (d) *Encyclopedia of Supramolecular Chemistry*; Atwood, J. L., Steed, J. W., Eds.; Taylor & Francis: New York, 2004. (e) Schneider, H. J. *Angew. Chem., Int. Ed.* **2009**, *48*, 3924−3977. (f) Salonen, L. M.; Ellermann, M.; Diederich, F. *Angew. Chem., Int. Ed.* **2011**, *50*, 4808−4842.

(2) (a) Conn, M. M.; Rebek, J., Jr. *Chem. Rev.* **1997**, *97*, 1647−1668. (b) Cram, D. J.; Cram, J. M. *Container Molecules and Their Guests*; The Royal Society of Chemistry: Cambridge, 1997. (c) Jasat, A.; Sherman, J. C. *Chem. Rev.* **1999**, *99*, 931−968.

(3) (a) Gabard, J.; Collet, A. *J. Chem. Soc., Chem. Commun.* **1981**, 1137−1139. (b) Collet, A. *Tetrahedron* **1987**, *43*, 5725−5759. (c) Brotin, T.; Dutasta, J.-P. *Chem. Rev.* **2009**, *109*, 88−130.

(4) (a) Canceill, J.; Cesario, M.; Collet, A.; Guilhem, J.; Lacombe, L.; Lozach, B.; Pascard, C. *Angew. Chem., Int. Ed. Engl.* **1989**, *28*, 1246−1248. (b) Garel, L.; Dutasta, J. P.; Collet, A. *Angew. Chem., Int. Ed.*

DOI: 10.1021/acs.joc.5b01187
J. Org. Chem. 2015, 80, 8065−8072

Engl. **1993**, *32*, 1169−1171. (c) Bartik, K.; Luhmer, M.; Dutasta, J.-P.; Collet, A.; Reisse, J. *J. Am. Chem. Soc.* **1998**, *120*, 784−791.
(5) (a) Sears, D. N.; Jameson, C. J. *J. Chem. Phys.* **2003**, *119*, 12231−12244. (b) Bagno, A.; Saielli, G. *Chem. - Eur. J.* **2012**, *18*, 7341−7345. (c) Dubost, E.; Dognon, J.-P.; Rousseau, B.; Milanole, G.; Dugave, C.; Boulard, Y.; Léonce, E.; Boutin, C.; Berthault, P. *Angew. Chem., Int. Ed.* **2014**, *53*, 9837−9840.
(6) Haberhauer, G.; Pintér, Á.; Woitschetzki, S. *Nat. Commun.* **2013**, *4*, 2945.
(7) Rekharsky, M.; Inoue, Y. *Encyclopedia of Supramolecular Chemistry*; Atwood, J. L., Steed, J. W., Eds.; Taylor & Francis: New York, 2004.
(8) Haberhauer, G.; Woitschetzki, S.; Bandmann, H. *Nat. Commun.* **2014**, *5*, 3542.
(9) (a) Purse, B. W.; Rebek, J. *Proc. Natl. Acad. Sci. U. S. A.* **2006**, *103*, 2530−2534. (b) Ajami, D.; Rebek, J. *Nat. Chem.* **2009**, *1*, 87−90. (c) Rebek, J., Jr *Acc. Chem. Res.* **2009**, *42*, 1660−1668. (d) Ajami, D.; Rebek, J. *Acc. Chem. Res.* **2012**, *46*, 990−999.
(10) (a) Ajami, D.; Liu, L.; Rebek, J., Jr. *Chem. Soc. Rev.* **2015**, *44*, 490−499. (b) Assaf, K. I.; Nau, W. M. *Chem. Soc. Rev.* **2015**, *44*, 394−418. (c) Ballester, P.; Fujita, M.; Rebek, J., Jr. *Chem. Soc. Rev.* **2015**, *44*, 392−393. (d) Dumitrescu, D.; Legrand, Y.-M.; Petit, E.; van der Lee, A.; Barboiu, M. *Chem. Sci.* **2015**, *6*, 2079−2086. (e) Hermann, K.; Ruan, Y.; Hardin, A. M.; Hadad, C. M.; Badjic, J. D. *Chem. Soc. Rev.* **2015**, *44*, 500−514. (f) Kim, D. S.; Sessler, J. L. *Chem. Soc. Rev.* **2015**, *44*, 532−546. (g) Kobayashi, K.; Yamanaka, M. *Chem. Soc. Rev.* **2015**, *44*, 449−466. (h) Leenders, S. H.; Gramage-Doria, R.; de Bruin, B.; Reek, J. N. *Chem. Soc. Rev.* **2015**, *44*, 433−448. (i) Zarra, S.; Wood, D. M.; Roberts, D. A.; Nitschke, J. R. *Chem. Soc. Rev.* **2015**, *44*, 419−432.
(11) Lide, D. R.; Haynes, W. M. *CRC Handbook of Chemistry and Physics*; CRC Press: Boca Raton, 2009.
(12) Canceill, J.; Lacombe, L.; Collet, A. *J. Am. Chem. Soc.* **1986**, *108*, 4230−4232.
(13) Chaffee, K. E.; Fogarty, H. A.; Brotin, T.; Goodson, B. M.; Dutasta, J.-P. *J. Phys. Chem. A* **2009**, *113*, 13675−13684.
(14) (a) Haberhauer, G.; Rominger, F. *Eur. J. Org. Chem.* **2003**, *2003*, 3209−3218. (b) Haberhauer, G.; Oeser, T.; Rominger, F. *Chem. Commun.* **2004**, 2044−2045.
(15) Frisch, M. J.et al. *Gaussian 09*, Revision A.02; Gaussian, Inc.: Wallingford, CT, 2009.
(16) *TURBOMOLE V6.3 2011*; University of Karlsruhe and Forschungszentrum Karlsruhe GmbH: Karlsruhe, Germany, 2011.
(17) Becke, A. D. *Phys. Rev. A: At., Mol., Opt. Phys.* **1988**, *38*, 3098−3100.
(18) Lee, C.; Yang, W.; Parr, R. G. *Phys. Rev. B: Condens. Matter Mater. Phys.* **1988**, *37*, 785−789.
(19) Miehlich, B.; Savin, A.; Stoll, H.; Preuss, H. *Chem. Phys. Lett.* **1989**, *157*, 200−206.
(20) Grimme, S.; Antony, J.; Ehrlich, S.; Krieg, H. *J. Chem. Phys.* **2010**, *132*, 154104.
(21) Grimme, S. *Chem. - Eur. J.* **2012**, *18*, 9955−9964.
(22) (a) Ditchfield, R.; Hehre, W. J.; Pople, J. A. *J. Chem. Phys.* **1971**, *54*, 724−728. (b) Hehre, W. J.; Ditchfield, R.; Pople, J. A. *J. Chem. Phys.* **1972**, *56*, 2257−2261.
(23) (a) Dunning, T. H., Jr. *J. Chem. Phys.* **1989**, *90*, 1007−1023. (b) Kendall, R. A.; Dunning, T. H., Jr.; Harrison, R. J. *J. Chem. Phys.* **1992**, *96*, 6796−6806.
(24) (a) Schäfer, A.; Horn, H.; Ahlrichs, R. *J. Chem. Phys.* **1992**, *97*, 2571−2577. (b) Weigend, F.; Ahlrichs, R. *Phys. Chem. Chem. Phys.* **2005**, *7*, 3297−3305.
(25) (a) Grimme, S. *J. Chem. Phys.* **2006**, *124*, 034108. (b) Schwabe, T.; Grimme, S. *Phys. Chem. Chem. Phys.* **2007**, *9*, 3397−3406.
(26) Klamt, A.; Schüürmann, G. *J. Chem. Soc., Perkin Trans. 2* **1993**, *2*, 799−805.
(27) Marenich, A. V.; Cramer, C. J.; Truhlar, D. G. *J. Phys. Chem. B* **2009**, *113*, 6378−6396.
(28) Klamt, A. *J. Phys. Chem.* **1995**, *99*, 2224−2235.
(29) Connolly, M. L. *J. Mol. Graphics* **1993**, *11*, 139−141.
(30) Mecozzi, S.; Rebek, J., Jr *Chem. - Eur. J.* **1998**, *4*, 1016−1022.
(31) (a) Gibb, C. L. D.; Gibb, B. C. *Chem. Commun.* **2007**, 1635−1637. (b) Gan, H.; Gibb, B. C. *Chem. Commun.* **2013**, *49*, 1395−1397. (c) Jordan, J. H.; Gibb, B. C. *Chem. Soc. Rev.* **2015**, *44*, 547−585.

DOI: 10.1021/acs.joc.5b01187
J. Org. Chem. 2015, 80, 8065−8072